Electronic Supplementary Material (ESI) for Journal of Materials Chemistry C.
This journal is © The Royal Society of Chemistry 2023

Supporting Information

Bluish-green-to-green thermally activated delayed fluorescent emitters based on β-diketone derivatives exhibiting a horizontal emission dipole orientation ratio of 88% and an external quantum efficiency of nearly 25%

Keigo Hoshi, [1] *Hisahiro Sasabe,** [1,2,3] *Ryoma Sato,* [1] *Naoto Yoshida,* [1] *Misaki Matsuya,* [1] *Yudai Chiba,* [1] *and Junji Kido* [1,2,3]

[1]Department of Organic Materials Science, Yamagata University, 4-3-16 Jonan, Yonezawa, Yamagata 992-8510, Japan, [2]Research Center of Organic Electronics (ROEL), Yamagata University, 4-3-16 Jonan, Yonezawa, Yamagata 992-8510, Japan, and [3]Frontier Center for Organic Materials (FROM), Yamagata University, 4-3-16 Jonan, Yonezawa, Yamagata 992-8510, Japan

*Corresponding author
E-mail: h-sasabe@yz.yamagata-u.ac.jp

General Considerations

Quantum chemical calculations were performed using the hybrid DFT functional Becke and Hartree-Fock exchange and Lee Yang and Parr correlation (B3LYP) and PBE0 as implemented by the Gaussian 09 program packages.[1] Electrons were described by the 6-31G(d) and def2SV basis sets for molecular structure optimization and single-point energy calculations, respectively. ^{1}H NMR and ^{13}C NMR spectra were recorded on JEOL 600 (600MHz) as pectrometer. Mass spectrum was obtained using a JEOL JMS-K9 mass spectrometer. DSC was performed using a Perkin-Elmer Diamond DSC Pyris instrument under nitrogen atmosphere at a heating rate of 10 ˚C min^{-1}. TGA was undertaken using a SEIKO EXSTAR 6000 TG/DTA 6200 unit under nitrogen atmosphere at a heating rate of 10 ˚C min^{-1}. UV–vis spectra was measred using a Shimadzu UV-2600 spectrophotometer. Photoluminescence spectra were measured using a FluoroMax-2 (Jobin-Yvon-Spex) luminescence spectrometer. The I_p was determined by a PYS under the vacuum (=10^{-3} Pa).[2] Transient PL decay curves and time resolved photoluminescence spectra were measured by using a streak camera (C4334 from Hamamatsu Photonics) at 300 K and 6 K. Photoluminescence quantum yield were measured using a Hamamatsu C11347 absolute PL quantum yield spectrometer with an integral sphere at an excitation wavelength of each sample. Natural transition orbitals (NTO) of $S_{1,2}$ and $T_{1\text{-}3}$ states were calculated using PBE0 functional with def2SV basis set. SOC matrix elements were calculated by using the Breit–Pauli Hamiltonian with an effective charge approximation implemented in the PySOC program[3] at the same level of theory.

Device Fabrication and Characterization

The substrates were cleaned with ultrapurified water and organic solvents, and then dry-cleaned for 30 minutes by exposure to UV–ozone. The organic layers were deposited onto the ITO substrates under the vacuum (=10^{-5} Pa), successively. LiF and Al was patterned using a shadow mask with an array of 2 mm × 2mm openings without breaking the vacuum (=10^{-5} Pa). The electroluminescent (EL) were taken using an optical multichannel analyzer Hamamatsu Photonics PMA-11. The current density–voltage and luminance–voltage characteristics were measured by using a Keithley source measure unit 2400 and a Minolta CS200 luminance meter, respectively.

[1] M. J. Frisch et al. Gaussian 09; Gaussian Inc.: Pittsburgh, PA 2009.

[2] H. Ishii, D. Tsunami, T. Suenaga, N. Sato, Y. Kumura, M. Niwano, *J. Surf. Sci. Jpn.* **2007**, *28*, 264.

[3] X. Gao, S. Bai, D. Fazzi, T. Niehaus, M. Barbatti, W. Thiel, *J. Chem. Theory Comput.* **2017**, *13*, 515.

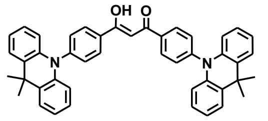

DMACPDO

Mw : 639
λ_{PL} : 524 nm/λ_{EL} : 536 nm
PLQY : 86%, τ_d : 1.94 μs, EQE_{max} : 23.9%
J. Am. Chem. Soc. **2018**, *140*, 8877.

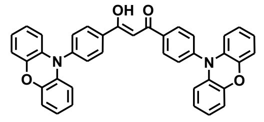

PXZPDO

Mw : 587
λ_{PL} : 552 nm/λ_{EL} : 560 nm
PLQY : 68%, τ_d : 1.33 μs, EQE_{max} : 18.8%
J. Am. Chem. Soc. **2018**, *140*, 8877.

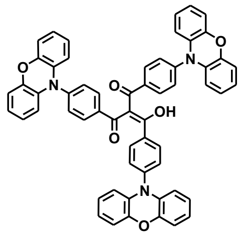

TPXZBM

Mw : 872
λ_{PL} : 578 nm/λ_{EL} : 582 nm
PLQY : 30%, τ_d : 1.44 μs, EQE_{max} : 12.7%
ACS Appl. Mater. Interf. **2021**, *13,* 15459.

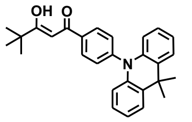

L-1

Mw : 412
λ_{PL} : 499 nm/λ_{EL} : 517 nm
PLQY : 24%, τ_d : 6.2 μs, EQE_{max} : 3.4%
Angew. Chem. **2021**, *133*, 6101.

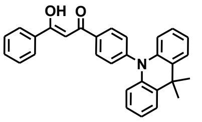

L-2

Mw : 432
λ_{PL} : 532 nm/λ_{EL} : 543 nm
PLQY : 38%, τ_d : 3.9 μs, EQE_{max} : 9.1%
Angew. Chem. **2021**, *133*, 6101.

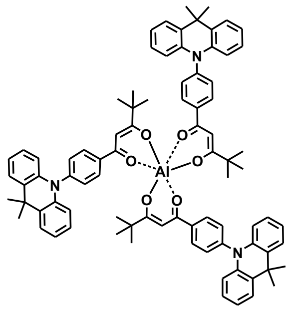

Al-1

Mw : 1259
λ_{PL} : 497 nm/λ_{EL} : 526 nm
PLQY : 65%, τ_d : 4.4 μs, EQE_{max} : 11.9%
Angew. Chem. **2021**, *133*, 6101.

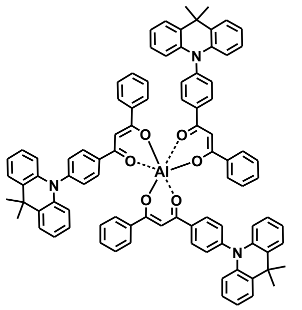

Al-2

Mw : 1319
λ_{PL} : 534 nm/λ_{EL} : 556 nm
PLQY : 79%, τ_d : 3.9 μs, EQE_{max} : 17.5%
Angew. Chem. **2021**, *133*, 6101.

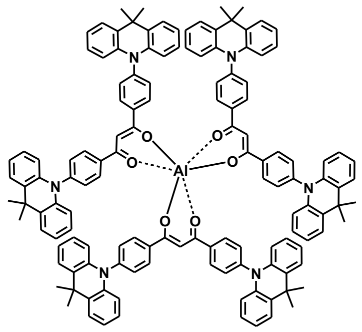

Al(DMACPDO)$_3$

Mw : 1940
λ_{PL} : 539 nm/λ_{EL} : 545 nm
PLQY : 100%, τ_d : 4.9 μs, EQE_{max} : 18.1%
Bull. Chem. Soc. Jpn. **2023**, *96,* 183.

Chart 1. Previous works on β-diketone based TADF emitters.

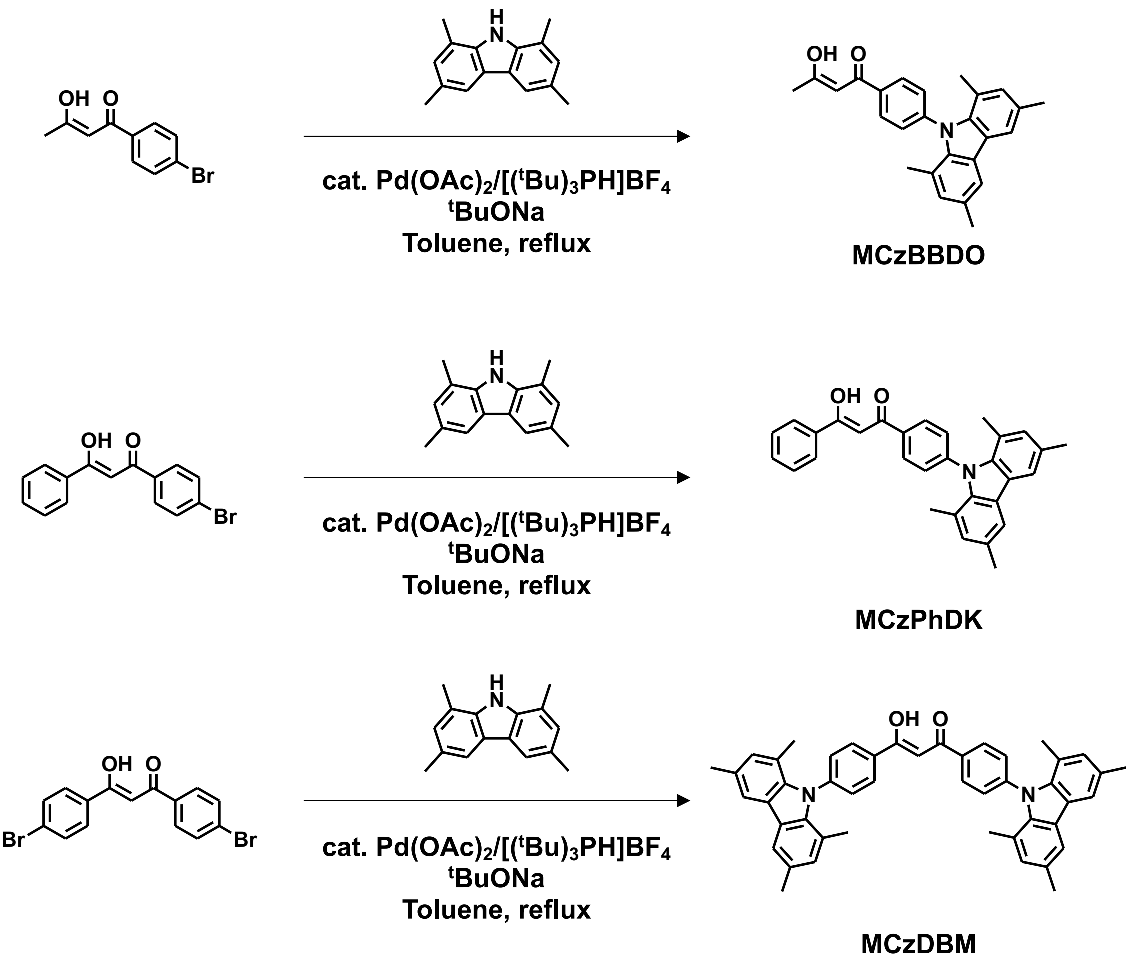

Scheme S1. Synthetic route of **MCzX** derivatives.

Synthesis of **MCzBBDO**

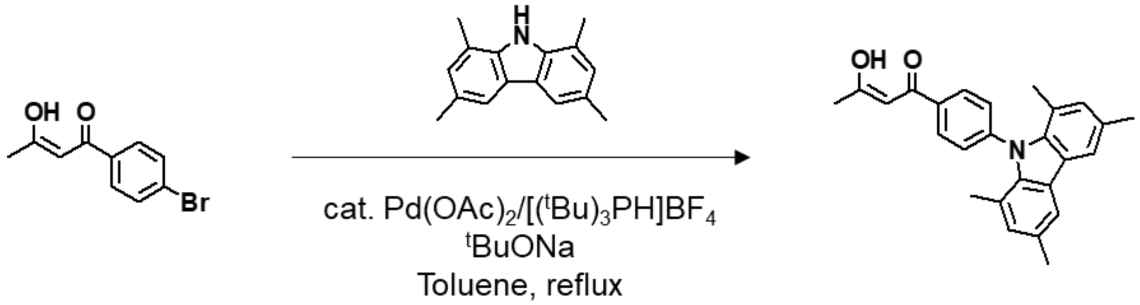

1-(4-Bromophenyl)-1,3-butanedione (1.2 g, 5 mmol), 1,3,6,8-tetramethyl-9*H*-carbazole (1.1 g, 5 mmol), and sodium *tert*-butoxide (1.4 g, 15 mmol) were added to a round bottom flask. Then, dry toluene (25 mL) was added and nitrogen was bubbled through the mixture for 60 minutes. Then, $Pd(OAc)_2$ (56 mg, 0.25 mmol) and $[(^tBu)_3PH]BF_4$ (218 mg, 0.75 mmol) were added and the resultant mixture was stirred 16 hours at reflux temperature under N_2 flow. The mixture was treated with 10% aqueous NH_4Cl and adjusted to pH 5 with hydrochloric acid. The aqueous phase was separated, and extracted with ethylacetate. The combined organic extracts were dried over anhydrous $MgSO_4$ and concentrated under reduced pressure. The resulting solid was purified by chromatography on silica gel (eluent: toluene) and recrystallized from toluene to afford MCzBBDO (1.3 g, 68%) as a light-yellow solid. : ^{1}H NMR (600 MHz, $CDCl_3$) δ = 16.16 (s, 1H), 7.96 (q, J = 2.7 Hz, 2H), 7.74 (s, 2H), 7.55 (q, J = 2.7 Hz, 2H), 6.91 (s, 2H), 6.28 (s, 1H), 2.47 (s, 6H), 2.25 (s, 3H), 1.86 (s, 6H) ppm ; ^{13}C-NMR (100 MHz, $CDCl_3$) δ = 194.2, 182.1, 146.2, 139.4, 135.0, 131.7, 131.5, 130.3, 129.3, 126.9, 124.4, 121.1, 117.9, 97.0, 26.0, 21.1, 19.5 ppm ; MS : m/z = 383 $[M+H]^+$; Anal. Calcd for $C_{26}H_{25}NO_2$: C, 81.43 ; H, 6.57 ; N, 3.65 %. Found : C, 81.44 ; H, 6.62 ; N, 3.65 %.

Synthesis of **MCzPhDK**

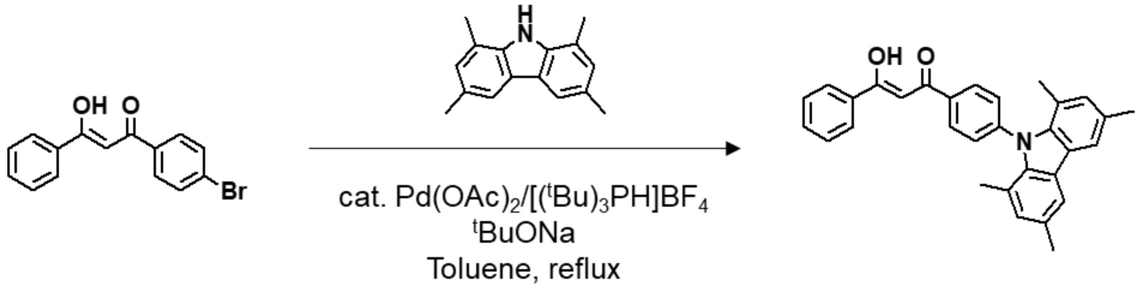

MCzPhDK was prepared according to the similar procedure using 1-(4-bromophenyl)-3-phenylpropane-1,3-dione. Yield: 73% as a yellow solid. ^{1}H NMR (600 MHz, $CDCl_3$) δ 16.89 (s, 1H), 8.08 (d, J = 8.1 Hz, 2H), 8.04-8.02 (m, 2H), 7.75 (s, 2H), 7.59 (dd, J = 11.1, 8.1 Hz, 3H), 7.52 (t, J = 7.6 Hz, 2H), 6.96 (s, 1H), 6.92 (s, 2H), 2.48 (s, 6H), 1.89 (s, 6H) ppm ; ^{13}C-NMR (100 MHz, $CDCl_3$) δ = 186.2, 184.4, 146.4, 139.4, 135.6, 135.4, 132.7, 131.6, 130.3, 129.3, 128.8, 127.2, 127.1, 124.4, 121.1, 117.9, 93.4, 21.1, 19.6 ppm ; MS : m/z = 445 $[M+H]^+$; Anal. Calcd for $C_{31}H_{27}NO_2$: C, 83.57 ; H, 6.11 ; N, 3.14 %. Found : C, 83.44 ; H, 6.22 ; N, 3.14 %.

Synthesis of **MCzDBM**

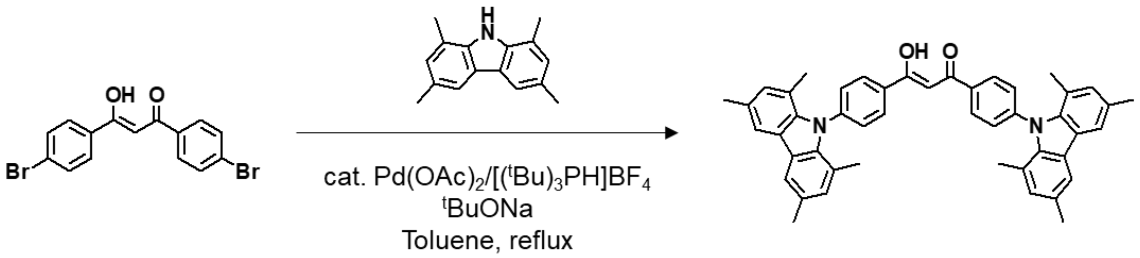

MCzDBM was prepared according to the similar procedure using 1,3-bis(4-bromophenyl)propane-1,3-dione. Yield: 88%. ^{1}H NMR (600 MHz, $CDCl_3$) δ 16.90 (s, 1H), 8.11 (d, J = 8.1 Hz, 4H), 7.75 (s, 4H), 7.62 (d, J = 8.1 Hz, 4H), 7.04 (s, 1H), 6.93 (s, 4H), 2.48 (s, 12H), 1.89 (s, 12H) ppm ; ^{13}C-NMR (100 MHz, $CDCl_3$) δ = 184.9, 146.7, 139.4, 135.5, 131.7, 130.3, 129.4, 127.2, 124.4, 121.1, 117.9, 93.8, 21.1, 19.6 ppm ; MS : m/z = 666 $[M+H]^+$; Anal. Calcd for $C_{47}H_{42}N_2O_2$: C, 84.65 ; H, 6.35 ; N, 4.20 %. Found : C, 84.74 ; H, 6.34 ; N, 4.20 %.

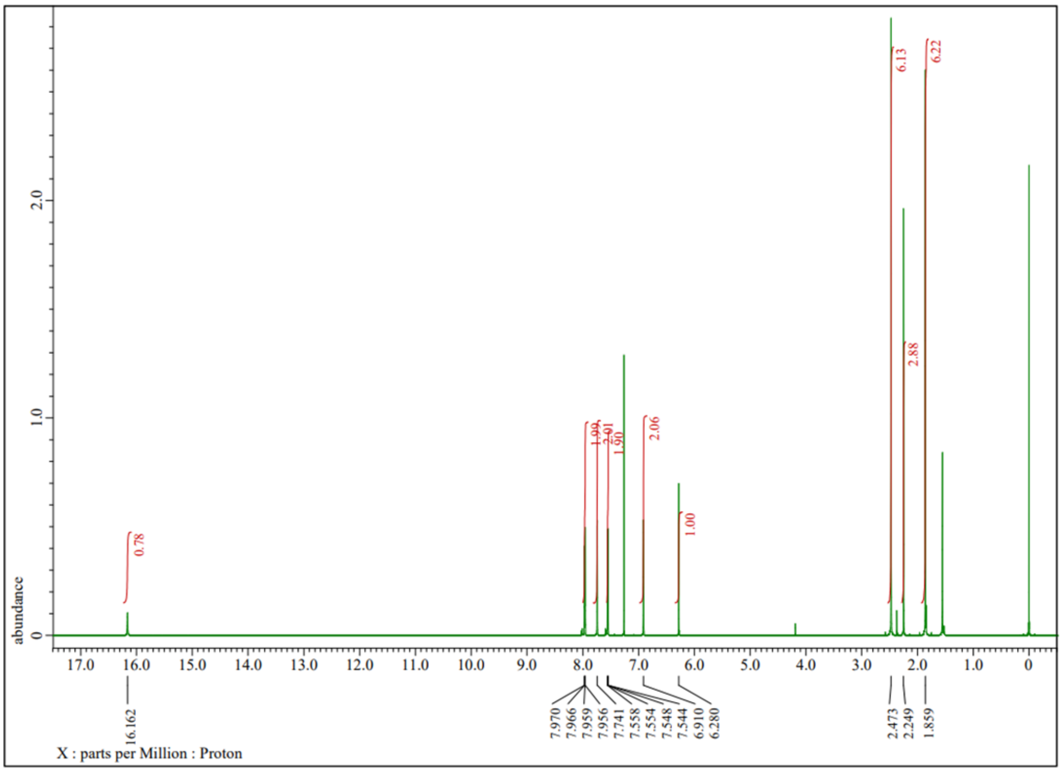

Figure S1. ^{1}H NMR spectrum of **MCzBBDO** (600 MHz, $CDCl_3$).

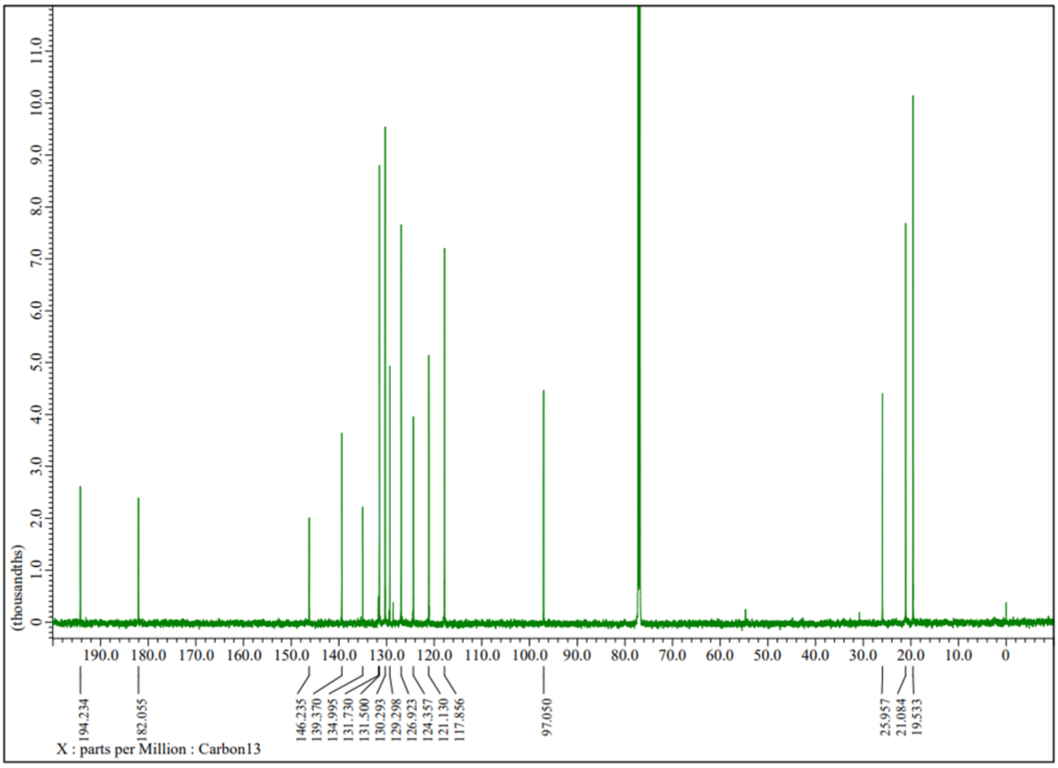

Figure S2. ^{13}C NMR spectrum of **MCzBBDO** (100 MHz, CDCl$_3$).

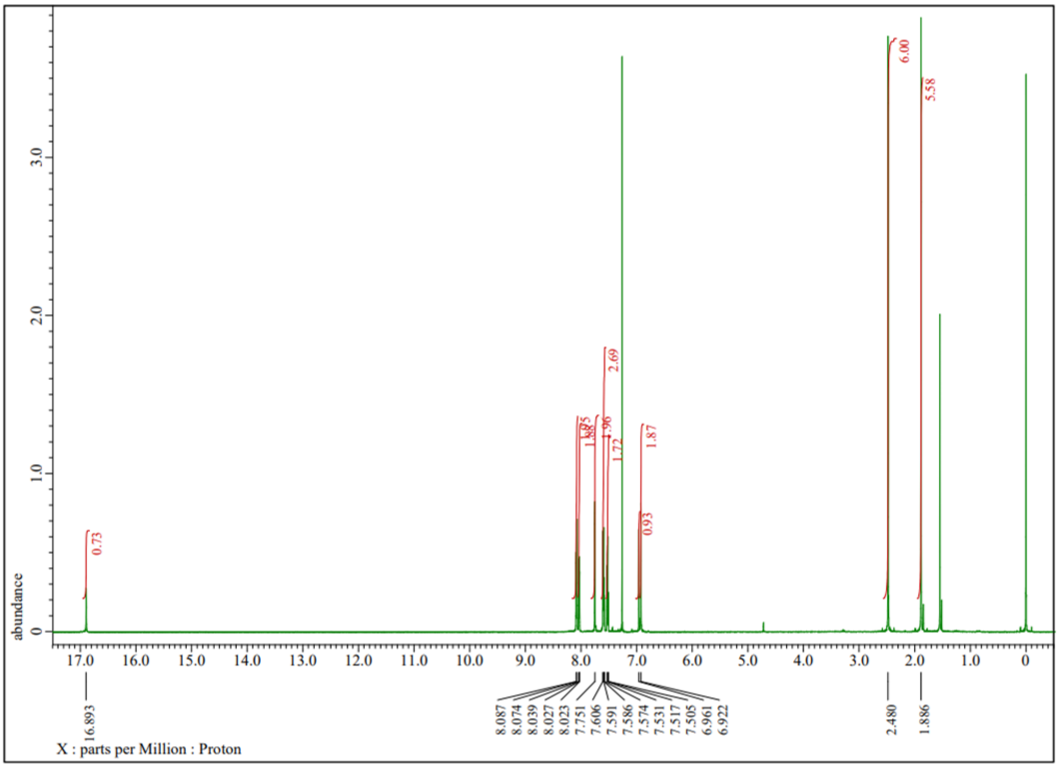

Figure S3. ^{1}H NMR spectrum of **MCzPhDK** (600 MHz, $CDCl_3$).

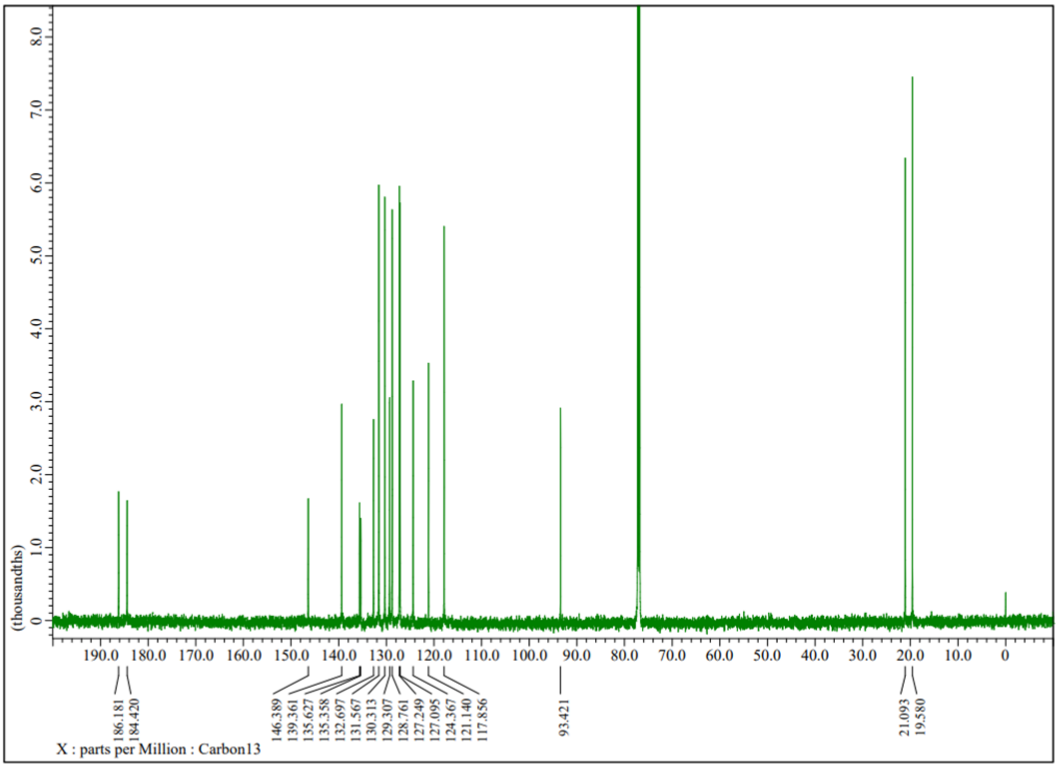

Figure S4. ^{13}C NMR spectrum of **MCzPhDK** (100 MHz, $CDCl_3$).

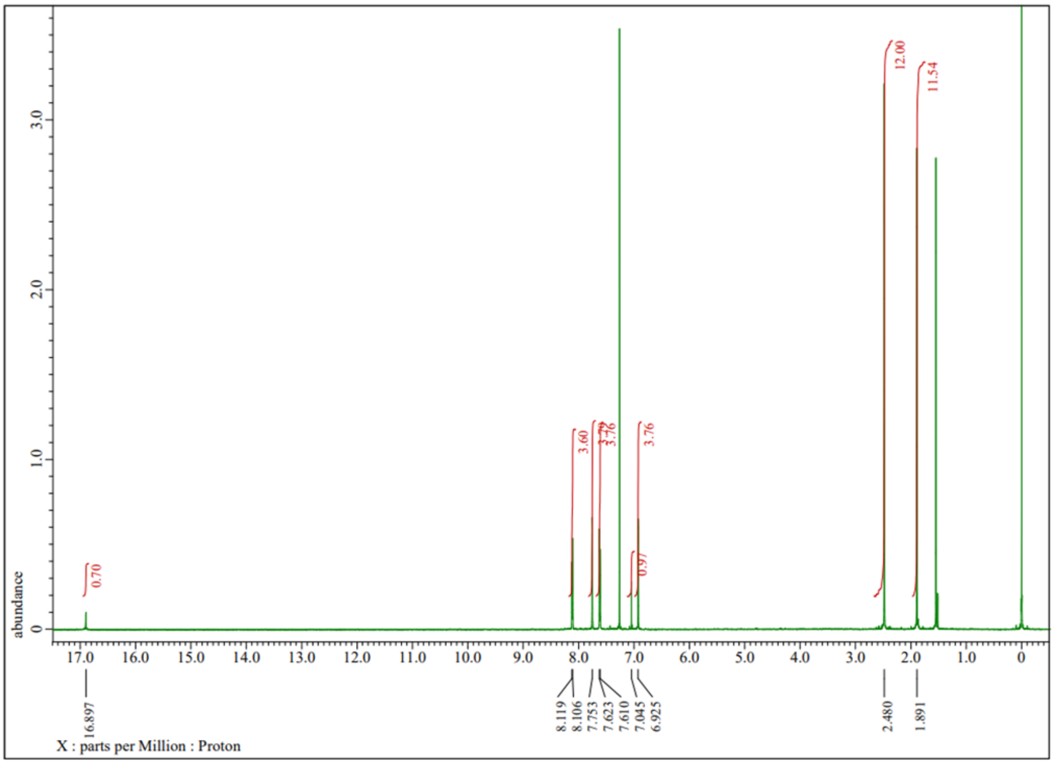

Figure S5. ^{1}H NMR spectrum of **MCzDBM** (600 MHz, $CDCl_3$).

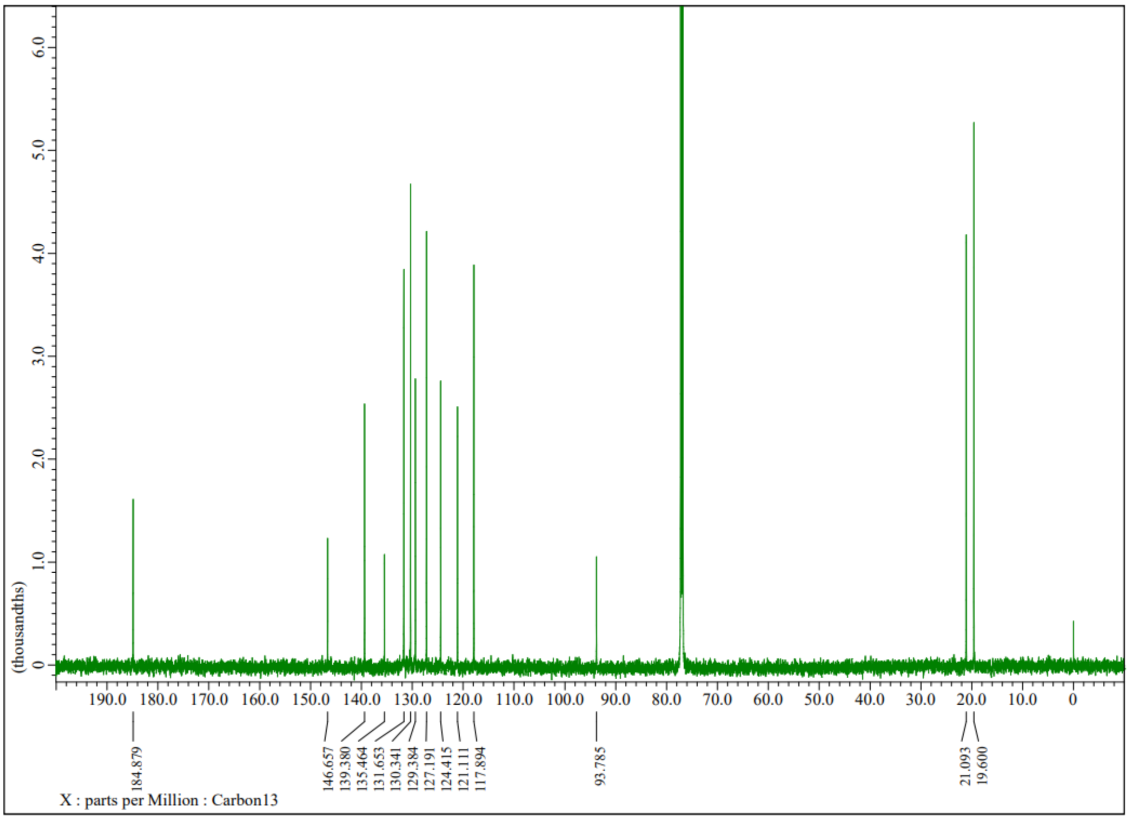

Figure S6. ^{13}C NMR spectrum of **MCzDBM** (100 MHz, $CDCl_3$).

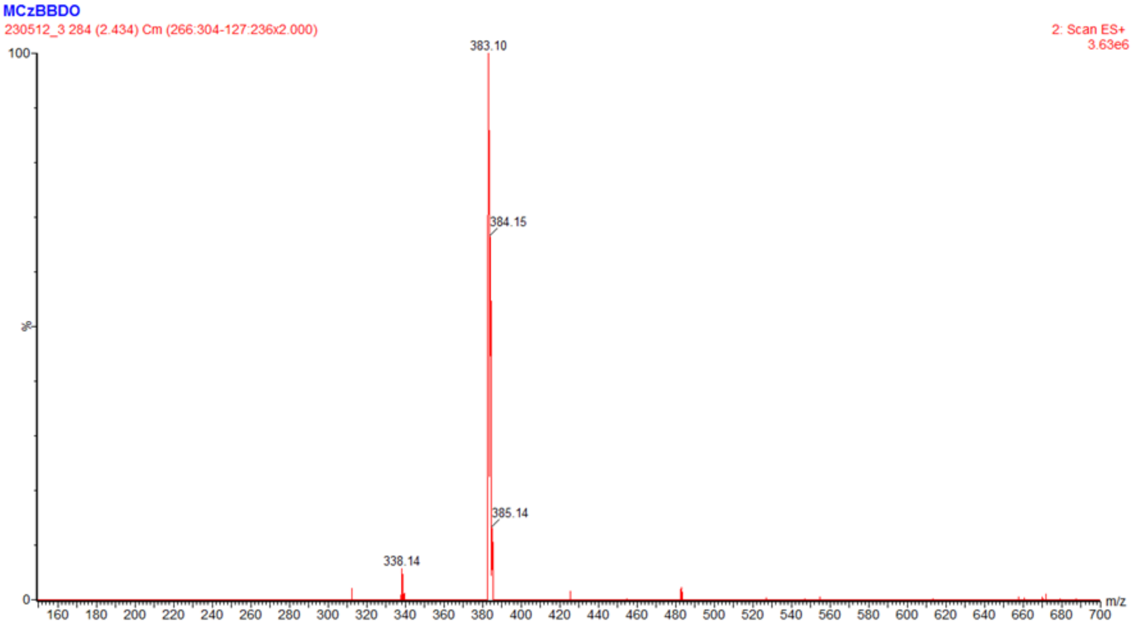

Figure S7. MS spectrum of **MCzBBDO.**

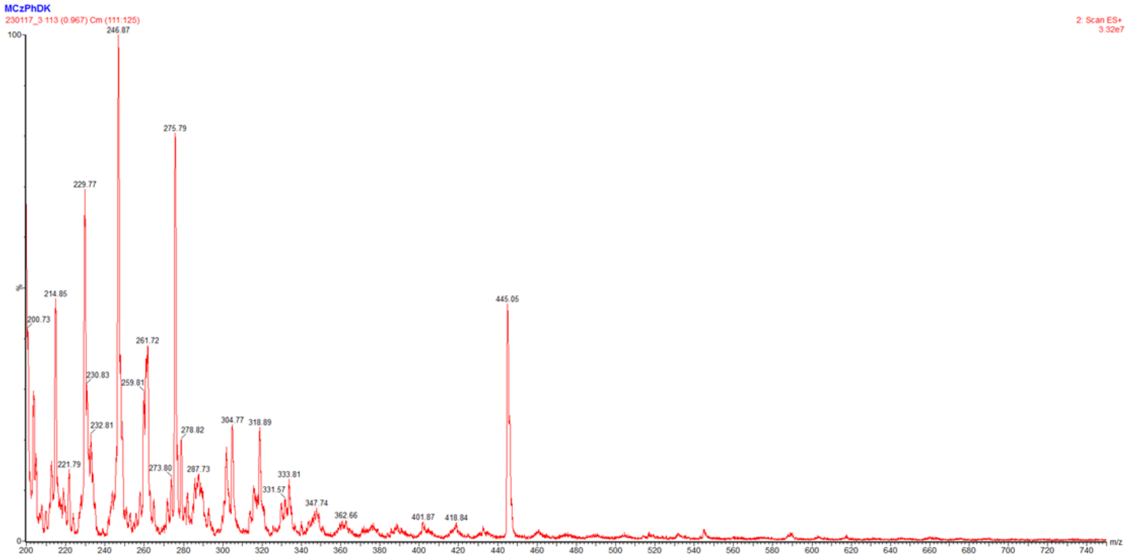

Figure S8. MS spectrum of **MCzPhDK.**

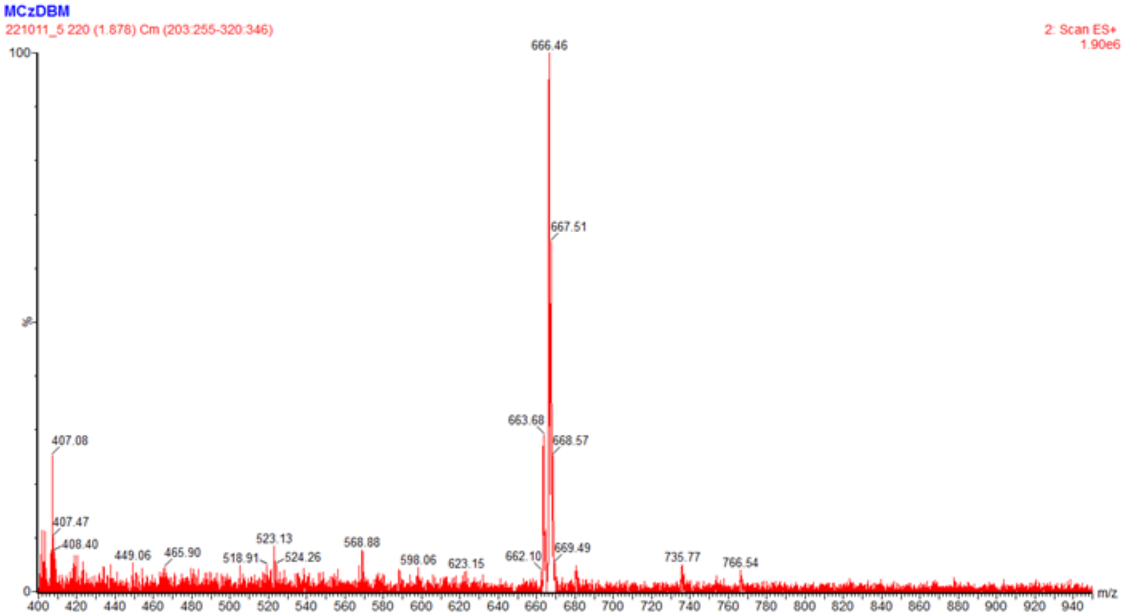

Figure S9. MS spectrum of **MCzDBM.**

Thermal property

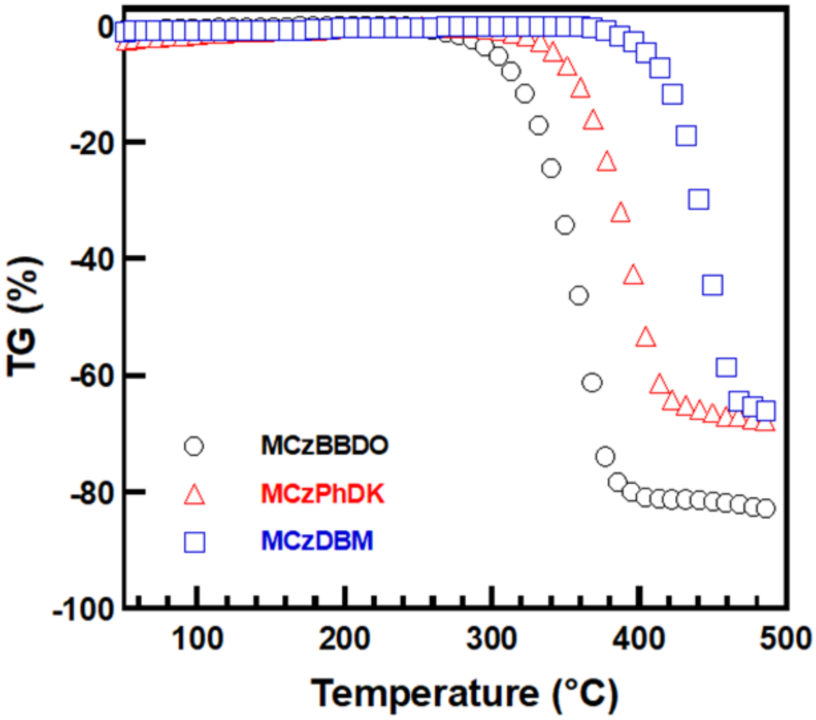

Figure S10. TGA curve of **MCzX derivatives**.

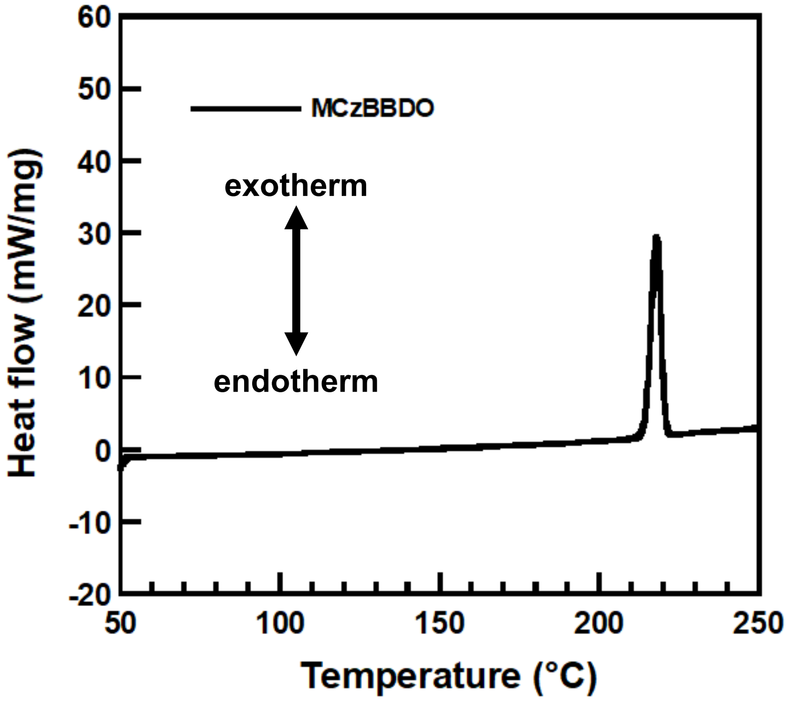

Figure S11. DSC curve of **MCzBBDO.**

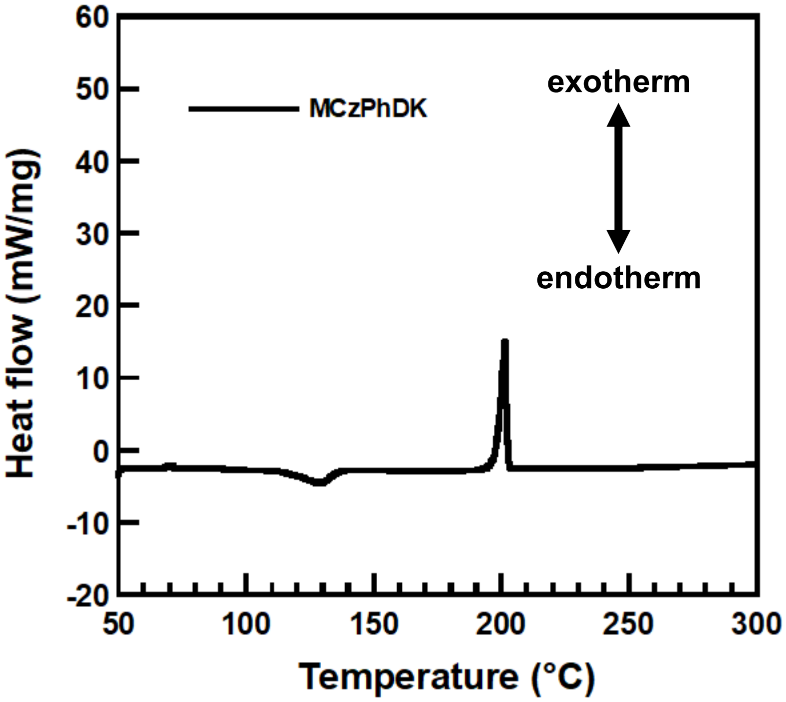

Figure S12. DSC curve of **MCzPhDK.**

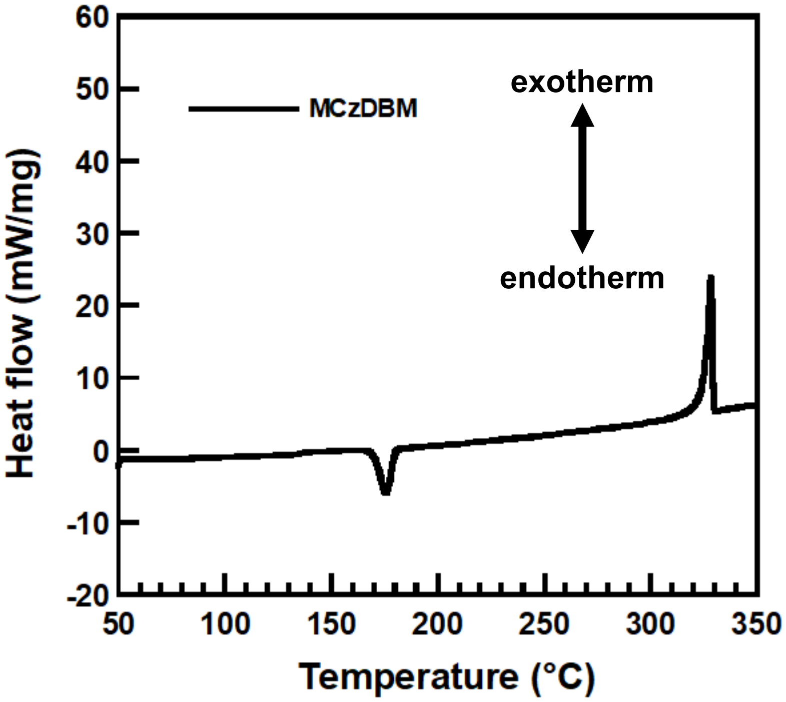

Figure S13. DSC curve of **MCzDBM.**

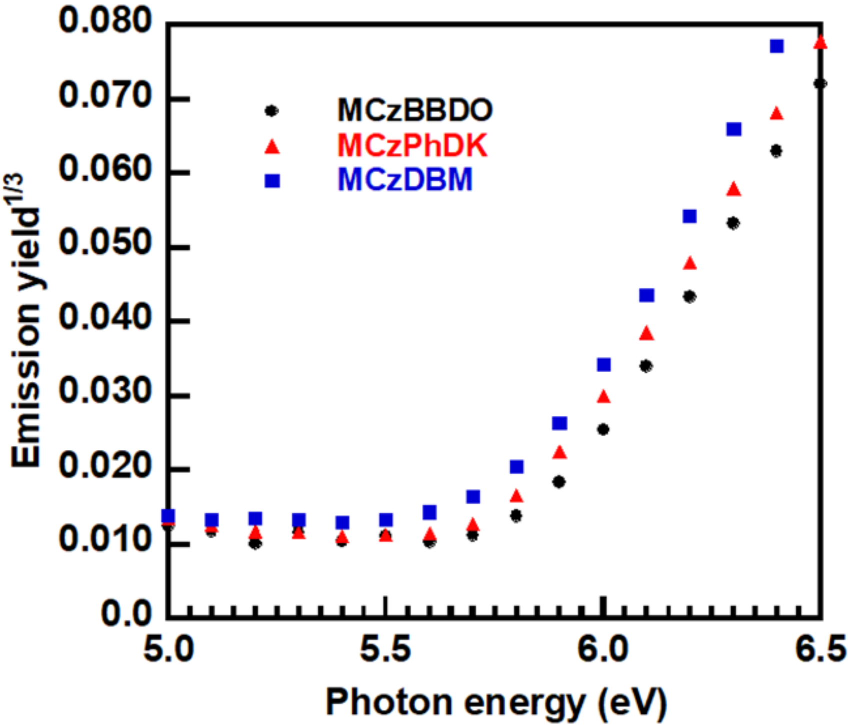

Figure S14. PYS spectra.

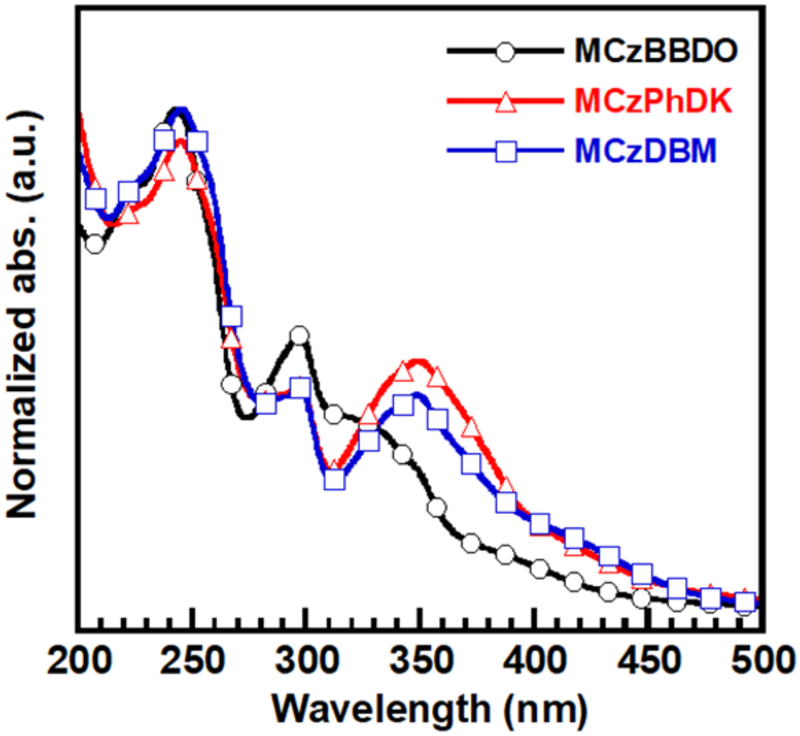

Figure S15. UV-vis absorption spectra of neat film (Thickness : 30 nm).

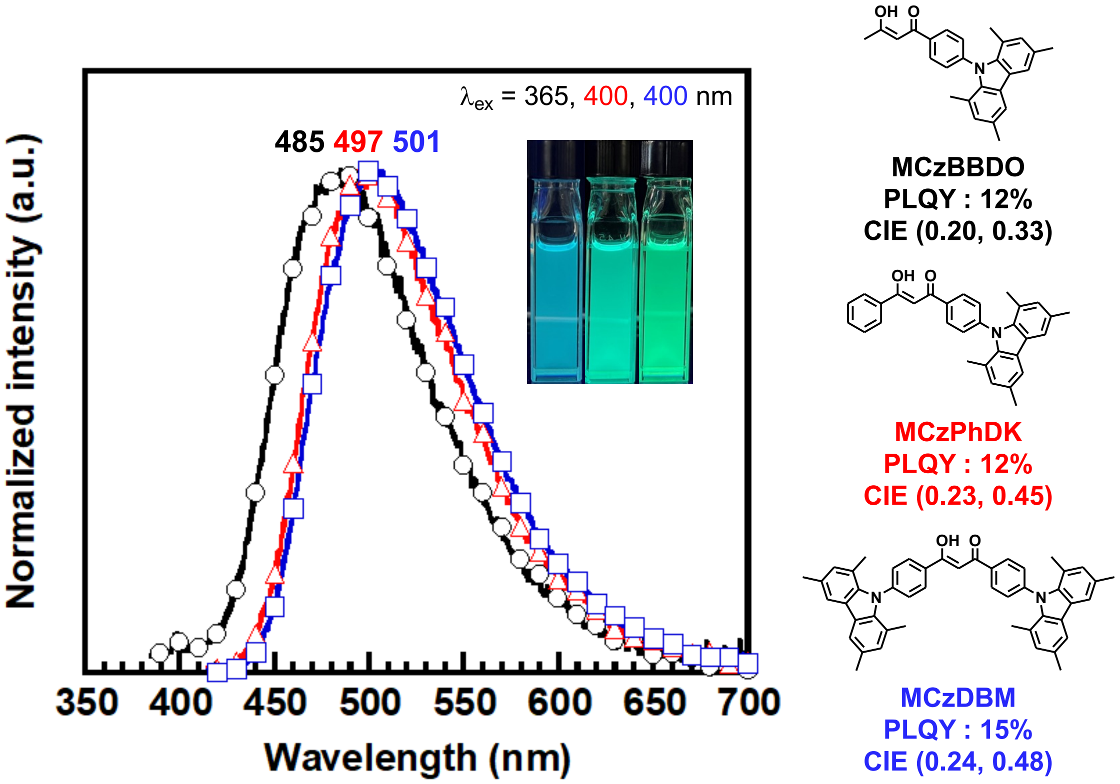

Figure S16. PL spectra in 10^{-5} M toluene solution.

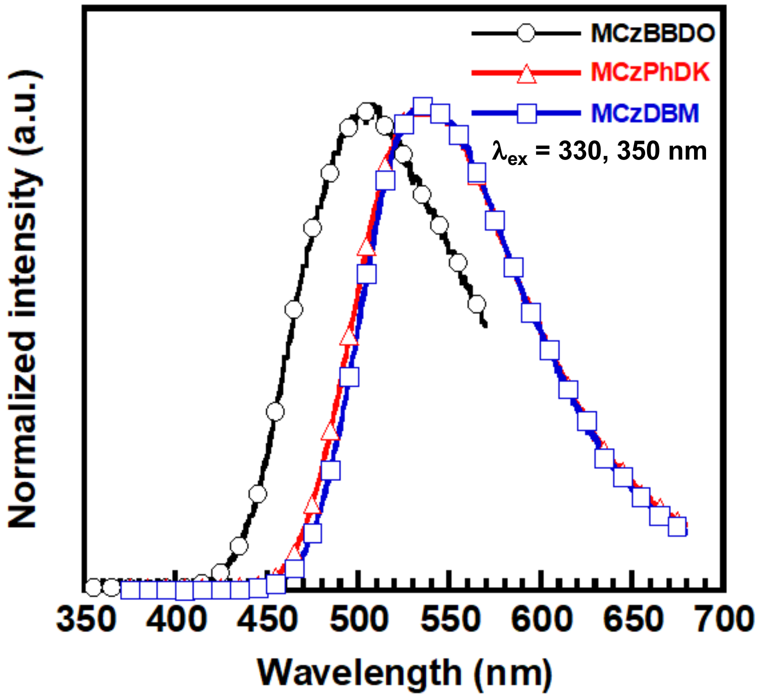

Figure S17. PL spectra of neat film (Thickness : 30 nm).

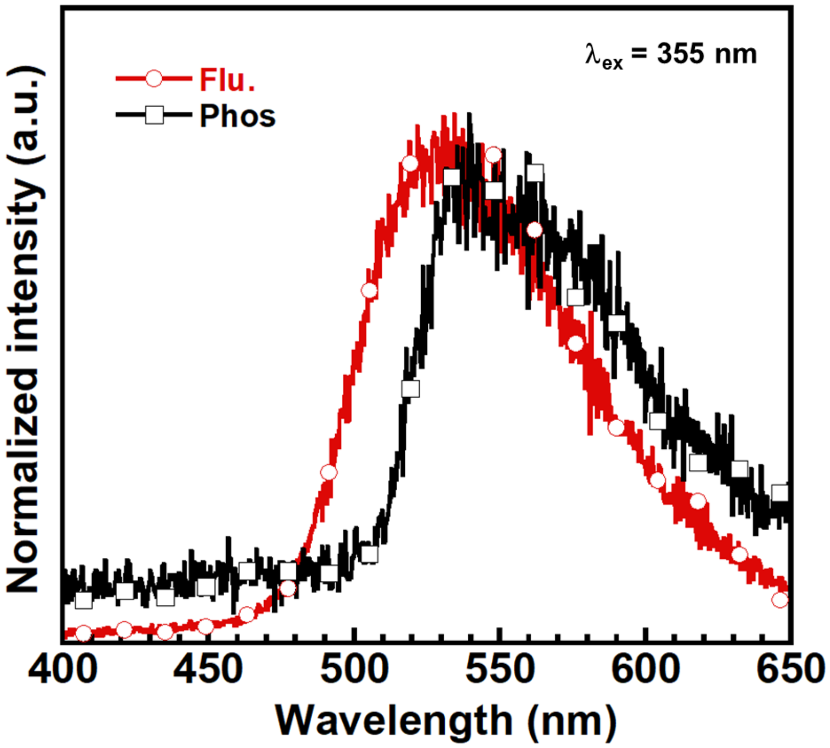

Figure S18. PL spectra of **MCzPhDK** in neat film (Thickness : 30 nm) at 6K.

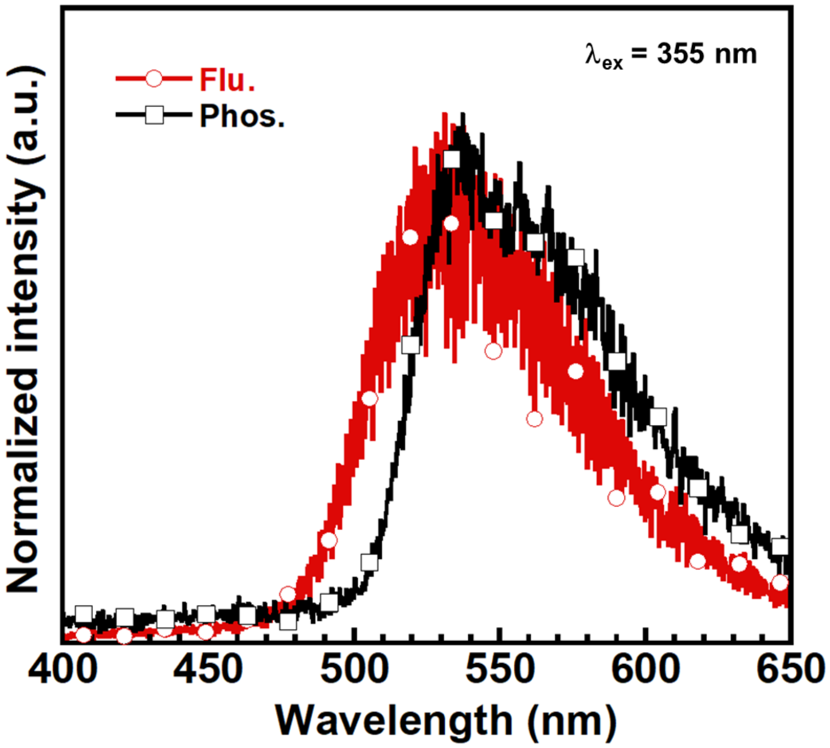

Figure S19. PL spectra of **MCzDBM** in neat film (Thickness : 30 nm) at 6K.

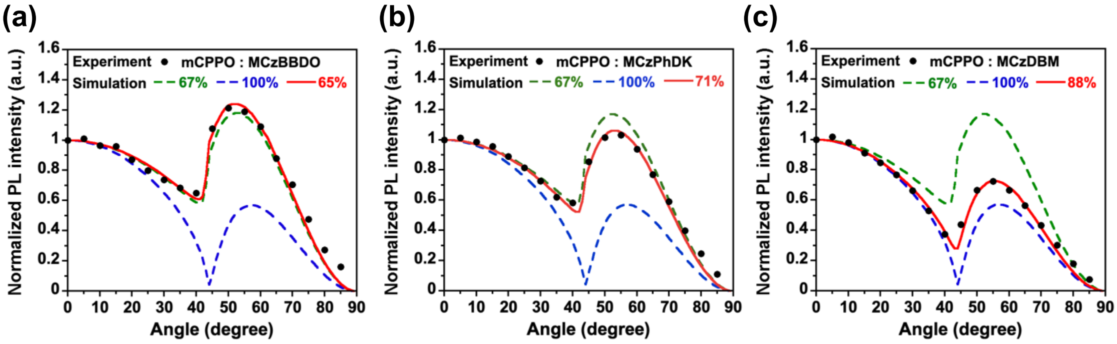

Figure S20. PL intensities of 3 wt% (a) **MCzBBDO**, (b) **MCzPhDK**, (c) **MCzDBM**-doped in **mCPPO** at different angles. The experimental data are compared with the fitting curve for different horizontal dipole orientations (Θ).

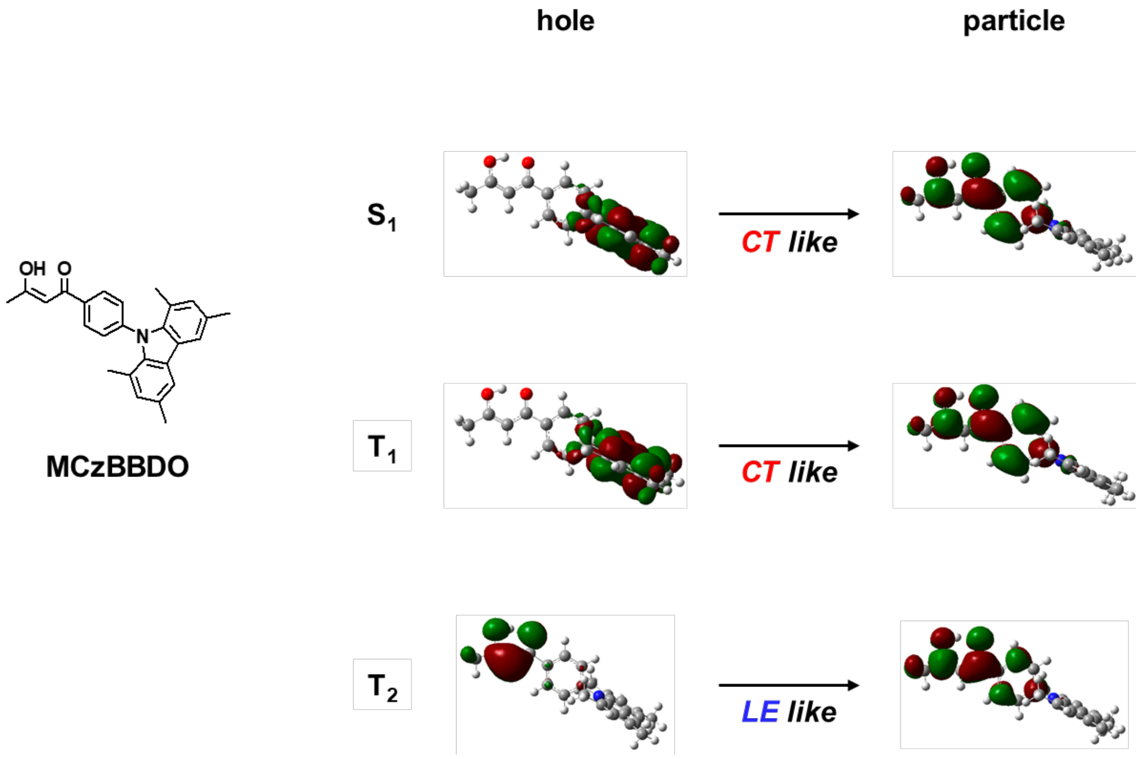

Figure S21. Representative NTOs of **MCzBBDO**.

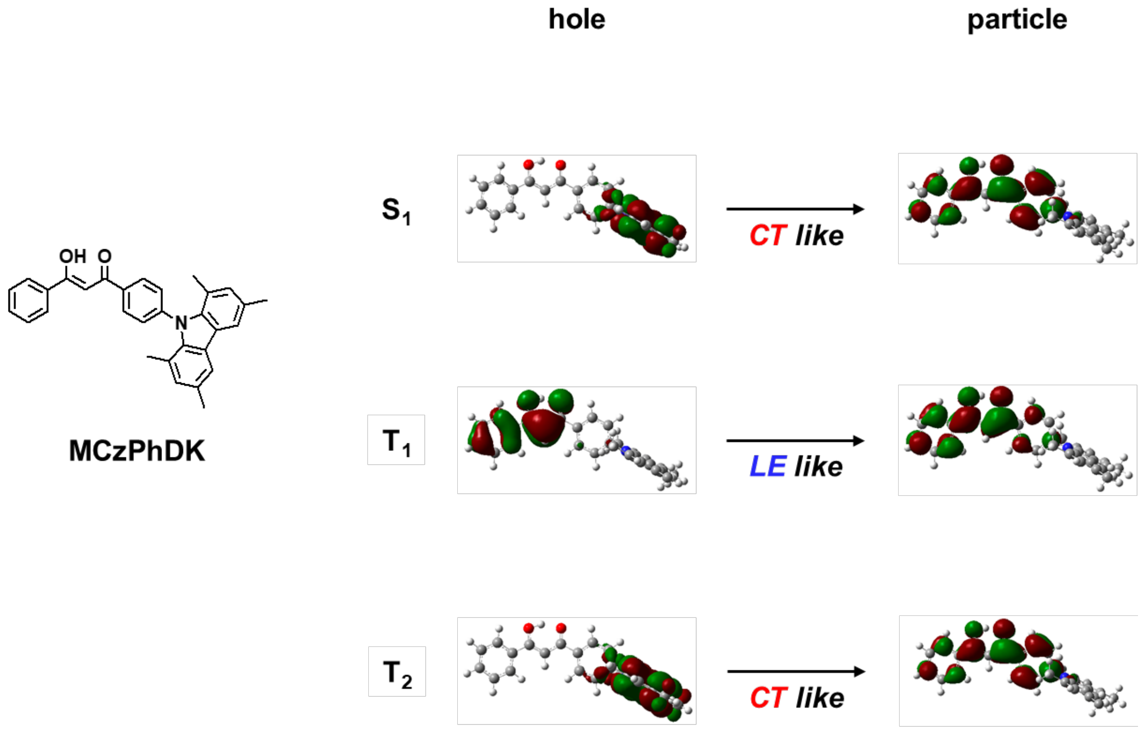

Figure S22. Representative NTOs of **MCzPhDK**.

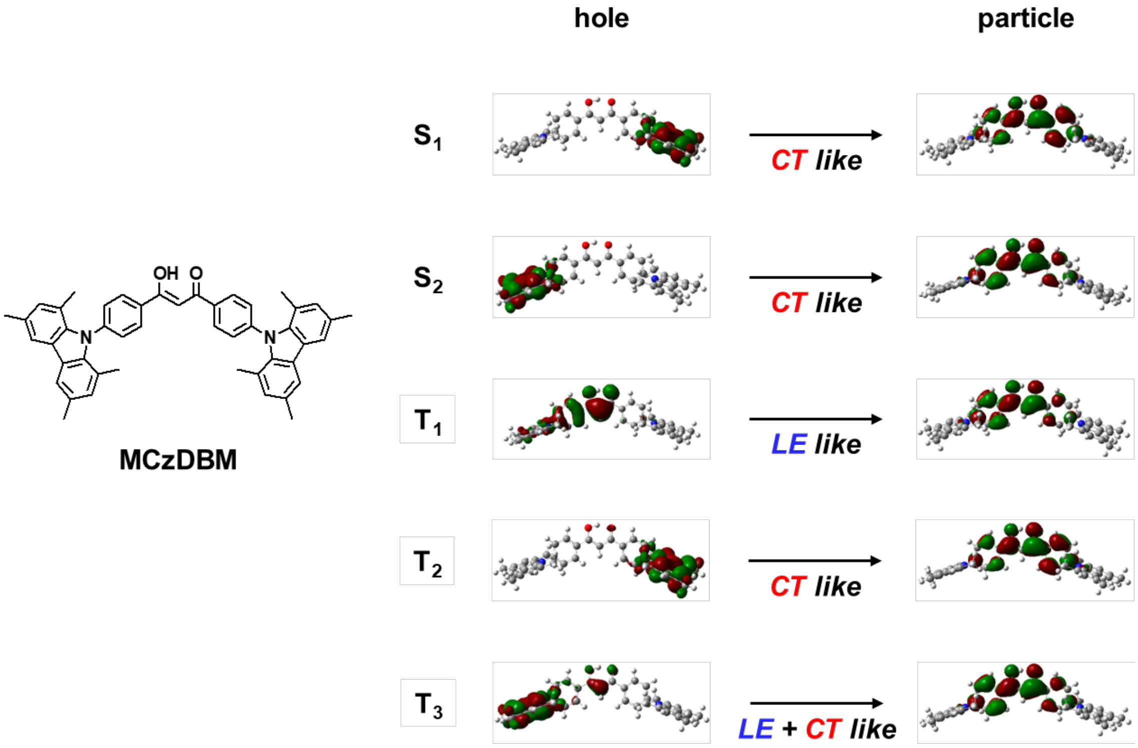

Figure S23. Representative NTOs of **MCzDBM**.

OLED perfoemances

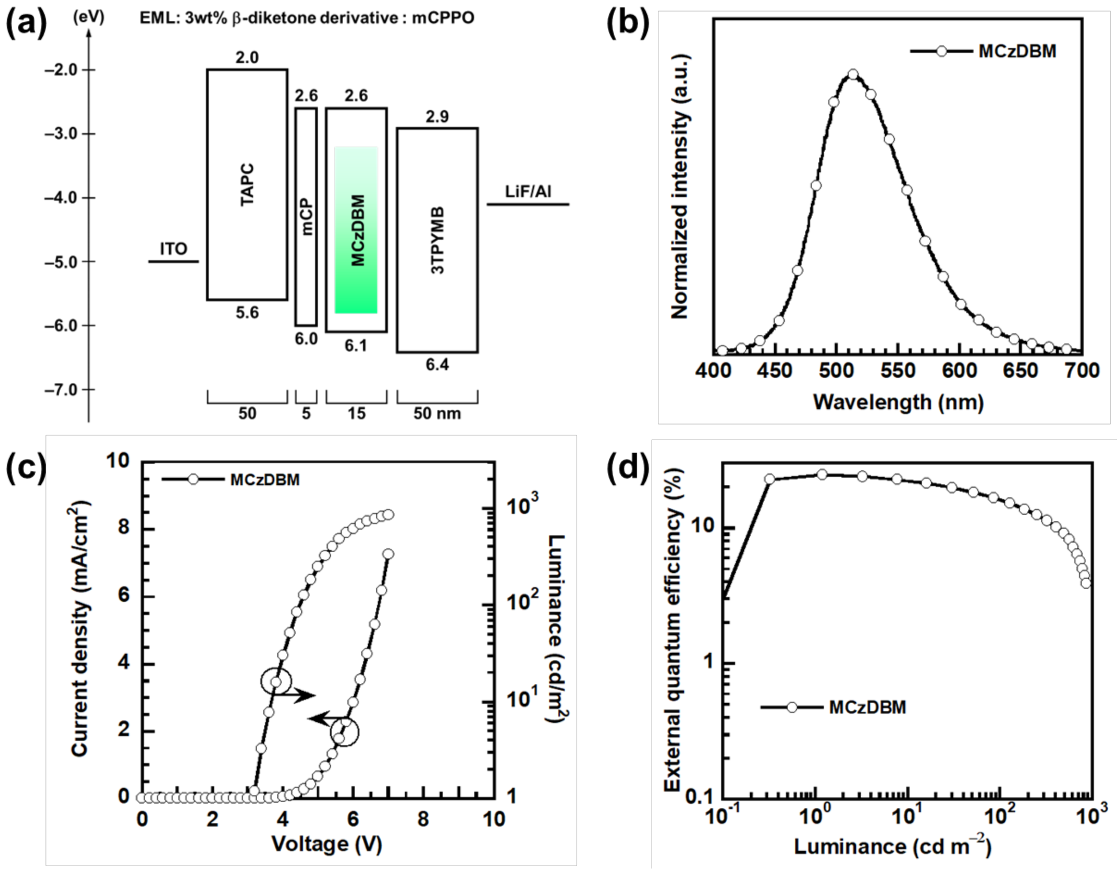

Figure S24. (a) Energy diagram of the device. Device performances of OLEDs: (b) EL spectra at 100 cd m^{-2}; (c) *J-V-L* characteristics; (d) *EQE-L* characteristics.

Photopysical properties, and rate constants

Rate constants were determined from the measurements of quantum yields and lifetimes of the fluorescence and TADF components according to the equations 1-4[4].

k_P $k_P = 1/\tau_P$ (1)

k_D $k_D = 1/\tau_D$ (2)

k_{ISC} $k_{ISC} = \Phi_D/(\Phi_P + \Phi_D)\ \tau_P$ (3)

k_{RISC} $k_{RISC} = (1/\tau_D)(\Phi_P + \Phi_D)/\Phi_D$ (4)

Table S1. Photophysical properties of 3 wt% emitter doped mCPPO films.

Compound	ΔE_{ST}[a] [eV]	Φ_{PL}[b] [%]	Φ_P[c] [%]	Φ_D[c] [%]	τ_P[d] [ns]	τ_D[d] [μs]	k_P[e] [10^8 s^{-1}]	k_D[e] [10^5 s^{-1}]	k_{ISC}[e] [10^8 s^{-1}]	k_{RISC}[e] [10^5 s^{-1}]
MCzBBDO	n.d.	21	12.1	8.5	6.1	66.8	1.6	0.15	1.4	0.12
MCzPhDK	0.12	39	21.0	17.5	4.8	13.9	2.1	0.72	1.6	0.76
MCzDBM	0.08	79	40.7	37.8	6.4	10.0	1.6	1.0	0.93	1.6

[a] These values were defined as the energy difference between E_S and E_T as obtained from the onset of fluorescence and the phosphorescence spectra of the neat film, respectively. [b] Absolute photoluminescence quantum yield. [c] Fluorescent and TADF components determined from the total Φ_{PL} and contribution of the integrated area of each component in the transient spectra to the total integrated area. [d] Lifetimes calculated from fluorescence decay. [e] Decay rates of fluorescence (k_P), Decay rates of delayed fluorescence (k_D), intersystem crossing from S_1 to T_1 (k_{ISC}), and reverse intersystem crossing from T_1 to S_1 (k_{RISC}) were calculated from Φ_{PL}, Φ_P, Φ_D, τ_P, and τ_D.

[4] F. B. Dias, T. J Penfold, A. P. Monkman, *Methods Appl. Fluoresc.* **2017**, *5*, 012001.